Hindawi
International Journal of Antennas and Propagation
Volume 2017, Article ID 1034673, 8 pages
https://doi.org/10.1155/2017/1034673

Research Article

A Model to Determine the Propagation Losses Based on the Integration of Hata-Okumura and Wavelet Neural Models

Luis F. Pedraza, Cesar A. Hernández, and Danilo A. López

Faculty of Technology and Engineering, Universidad Distrital Francisco José de Caldas, Bogotá, Colombia

Correspondence should be addressed to Luis F. Pedraza; pedrazaluis2001@gmail.com

Received 27 September 2016; Revised 26 December 2016; Accepted 2 February 2017; Published 22 February 2017

Academic Editor: Stefania Bonafoni

Radioelectric spectrum occupancy forecast has proven useful for the design of wireless systems able to harness spectrum opportunities like cognitive radio. This paper proposes the development of a model that identifies propagation losses and spectrum opportunities in a channel of a mobile cellular network for an urban environment using received signal power forecast. The proposed model integrates the Hata-Okumura (H-O) large-scale propagation model with a wavelet neural model. The model results, obtained through simulations, show that the wavelet neural model forecasts with a high degree of precision, which is consistent with the observed behavior in experiments carried out in wireless systems of this type.

1. Introduction

Radioelectric spectrum is regarded as a scarce asset. Nowadays, the use of a great percentage of licensed bands is low; and it has become normal to find frequency bands congested while others remain underutilized. In that context, cognitive radio (CR) has become a topic of increasing interest as a new paradigm seeking to optimize the use of radioelectric spectrum [1, 2]. A CR is an intelligent radio aware of the context, able to autonomously reconfigure itself to learn and adapt to radio environment [3]. Research on CR has been boosted by the interesting results obtained from the measuring campaigns made around the world [4–14], which show the underutilization of radioelectric spectrum in domains of frequency, time, and geographic distribution [5, 7–9, 11, 14].

One of the essentials from CR is that unlicensed users do not interfere with the activities of licensed users. A way to tackle this is by enabling unlicensed users to detect spectrum occupancy in different locations as a function of the environment considered and the propagation conditions, which provides an invaluable tool to the design, dimensioning, and evaluation of the performance in CR networks [15].

Propagation models were formulated in the late 1960s, with the intent of precisely estimate propagation losses in an environment. Initially, empirical and statistical propagation models were designed for urban areas [16, 17]. Later, in the early 1980s with the rise of mobile communications, propagation models were employed in micro- and macrocells scenarios [18–20], from which numerous efforts to understand and forecast the features of the channels in mobile communications have emerged [21].

Time series have been employed to propagation losses forecast. For example, neural networks have been used to forecast field strength [22], as well as average propagation losses [23, 24]. Another used method is fuzzy logic [25]. Also, the Seasonal Autoregressive Integrated Moving Average (SARIMA) and Generalized Autoregressive Conditional Heteroskedasticity (GARCH) are used for forecasting received power in wireless channels [26]. In this paper we develop a forecast of the received power in order to identify propagation losses and spectrum opportunities within a licensed mobile network integrating the H-O propagation model and the neuronal wavelet model in an urban environment.

This paper is structured as follows. In Section 2 the model is put forth. Section 3 presents and discusses the results of the received power and the duty cycle for the model studied. Section 4 shows the conclusions of the research.

2. Proposed Model

First the wavelet neural model was designed. Then, the H-O propagation model was adjusted using the measurements obtained from the urban environment. Finally, the proposed methodology to forecast spectrum opportunities is presented.

2.1. Wavelet Neural Model. For cognitive systems in [27] a backpropagation neural network is used to predict the state of the spectrum; also in [28, 29] a genetic algorithm was used to optimize the neural network. In [30] a neural network was utilized to forecast the power of television and GSM-900 bands. In [31], the spectrum is modeled and forecasted using the Daubechies wavelets. All the prior examples and those presented in [32, 33] portray the promising features of neural networks and wavelets to forecast the received power in wireless channels on models such as Markov and empirical mode decomposition-support vector regression. Therefore, in this paper we propose a theory combining wavelet and neural network [34] to improve forecasts of the received power in a channel of the technology Global System for Mobile Communications (GSM).

The input signal to the model that corresponds to the received power in a GSM channel for the measurements developed in [35] and analyzed in [32] can be decomposed using the Discrete Meyer (dmey) mother wavelet, which demonstrated a lower error when compared with the Daubechies, Coiflets, and Symlets mother wavelets [36]. The obtained results were two levels containing 4 coefficients. These coefficients are sent as an input of the wavelet multilayer neural network of backpropagation shown in Figure 1 and expressed as follows:

$$f[n] = g\sum_{i=1}^{n}\left[\frac{1}{\sqrt{M}}\sum_{k}W_{\Phi}[j_0;k]\,\Phi_{jo;k}[n] + \frac{1}{\sqrt{M}}\sum_{j=j_0}^{\infty}\sum_{k}W_{\psi}[j;k]\,\psi_{j;k}[n]\right], \quad (1)$$

where g is the activation function of the neural network, $f[n]$ is the sample projection in the time domain, $W_{\Phi}[j_0;k]$ are the approximation coefficients, $W_{\psi}[j;k]$ are the detailed coefficients, $\Phi_{jo,k}$ is the scale function, and $\psi_{j,k}$ is the translation function, which are discrete functions defined within $[0, M-1]$, for the total of M points.

The neural network in this case contains 2 inputs, 2 outputs, and 2 hidden layers. The network was initially trained with nearly five days of continuous measurements; and the number of training patterns was increased until the error decreased and turned relatively constant. This was achieved for 1000 training patterns. The output of the neural network was reconstructed using a wavelet analysis to obtain the forecast power, which had a training time that was satisfied with one day to achieve an acceptable error as indicated in [32].

2.2. Hata-Okumura Model. Figure 2 presents the environment of the Base Station (BS) used to carry out measurements with the spectrum analyzer in the north of Bogotá, Colombia. The six measurement spots correspond to the covering sites of the cell, located at different distances from BS, in order to evaluate and adjust the H-O propagation model [37]. The period of the measurements was of one hour approximately. The environment is flat and consists mainly of an important concentration of buildings; also, green zones and trees are present, as it can be seen in the measure spot D.

Table 1: BS parameters and spectrum analyzer.

Parameter	Value
BS transmission power (P_{TX})	26 dBm
BS height	26 m
BS antenna gain (G_{BS})	16.5 dBi
BS combiner losses (L_{co})	4 dB
BS cable losses (L_c)	4 dB
Analyzer antenna gain (G_{An})	3 dBi
Analyzer cable losses (L_{ca})	0.72 dB
Low-noise amplifier gain (G_{LNA})	11 dB
Analyzer height (A_H)	1.5 m
GSM channel transmission frequency (f_c)	828.93 MHz

Table 2: Propagation losses of the H-O model for the measurement spots in Figure 2.

Spot	$\overline{L}$ GSM channel (dB)
F (58 m)	82.282
C (152 m)	97.191
D (226 m)	103.329
B (287 m)	107.026
E (290 m)	107.187
A (328 m)	109.093

In Table 1 the parameters of the transmitter and receiver are presented, which are employed to evaluate the H-O propagation model. The model is then adjusted using the measured powers in the spots seen in Figure 2 [38].

Through (2) the theoretical average propagation losses ($\overline{L}$) are obtained of the H-O model for each measuring spot, as observed in Table 2:

$$\overline{L}\ (\text{dB}) = 69.55 + 26.16\log f_c - 13.82\log \text{hte} - a(h_{\text{re}}) + (44.9 - 6.55\log \text{hte})\log d, \quad (2)$$

where f_c is the carrier frequency in MHz, hte is the height of the transmitter antenna in m, h_{re} is the height of the receiver antenna in m, $a(h_{\text{re}})$ is the correction factor for the effective height of the mobile antenna, and d is the distance between the transmitter and receiver in km [37].

From the results of Table 2 and parameters in Table 1, the theoretical average received power ($\overline{P_{RX}}$) [39] is given by

$$\overline{P_{RX}} = P_{TX} + G_{BS} + G_{An} + G_{LNA} - \overline{L} - L_c - L_{co} - L_{ca}. \quad (3)$$

In Figure 3 $\overline{P_{RX}}$ is presented, obtained from (3) for the H-O model in comparison to the range of the measured received power with its respective average values. Figure 3 reveals a

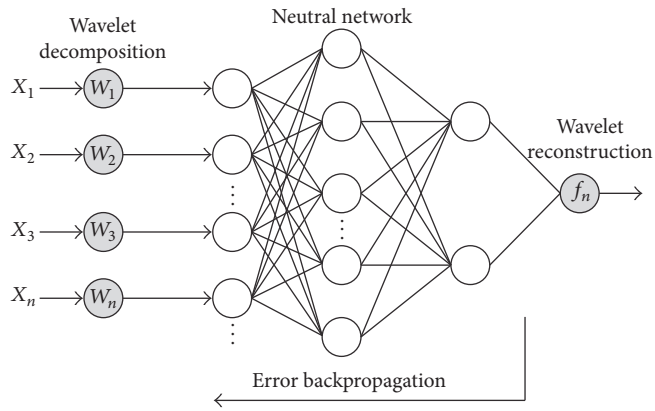

Figure 1: Wavelet neural network.

Figure 2: Measurement spots in north Bogotá, Colombia.

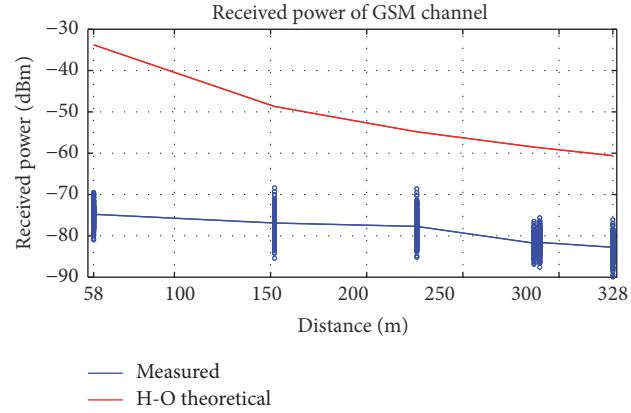

Figure 3: Theoretical and received power for the H-O model of the GSM channel.

significant difference between the theoretical data and the measured ones.

In order to increase H-O propagation model precision, the least squares method is employed [40] to adjust theoretical results to measured average values. From this, the following equation adjusted for the GSM channel is obtained:

$$\overline{L}\ (\mathrm{dB}) = 78.2616 + 26.16 \log f_c - 13.82 \log \mathrm{hte} - a\left(h_{\mathrm{re}}\right) + \left(19.5356 - 6.55 \log \mathrm{hte}\right) \log d. \quad (4)$$

Figure 4 presents the received power of the H-O model adjusted by (4) in regard to the average of the measured received power. In Figure 4 an approximation between the measured values and the adjusted model is shown, which has a mean squared error of 1.2688.

2.3. Proposed Methodology. In the following part the methodology to develop the proposed model and the general equation to forecast received power through the wavelet neural model and the H-O propagation model previously adjusted is described. The general procedure to obtain the forecasting model of spectrum opportunities in an unknown environment is shown below.

(1) Measuring. In this step the time-variant(s) channel(s) of the radioelectric spectrum is measured during a day, as described in [35].

(2) Adjusting the Propagation Model. The H-O propagation model is adjusted using, for example, the least squares method according to the average values of the measurements.

(3) Training of the Wavelet Neural Model. The measurements obtained at least within a 24-hour time frame are used to train the wavelet neural model designed.

(4) Integration of Models. Extrapolate the adjusted H-O propagation model to the wavelet neural model, thus integrating average propagation losses with instantaneous losses.

(5) Forecasting Received Power. Along the analyzed urban environment, received power is forecasted during a specified period of time using the compound model in step (4).

Therefore, the model that takes into consideration both instantaneous and average propagation losses can be described as follows:

$$L = \Delta L + \overline{L}, \quad (5)$$

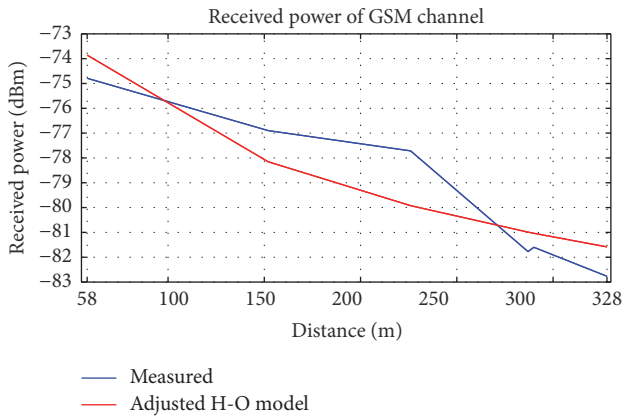

Figure 4: Adjusted and received power for H-O model of the GSM channel.

Table 3: Error variables for the received power forecasts in the GSM channel, based on the wavelet neural model.

	SMAPE	MAPE	MAE
GSM channel	0.0019	0.0010	0.1005

where $\Delta L = f(f[n])|_{f[n]=\Delta PRX}$ represent the instantaneous propagation losses according to the received power obtained using (1) and $\overline{L}$ are the average propagation losses obtained from the adjustment of (2) of the H-O model. Thus, combining (1) and (3), the received power is obtained as a function of the H-O model:

$$P_{RX} = g\sum_{i=1}^{n}\left[\frac{1}{\sqrt{M}}\sum_{k}W_{\Phi}\left[j_0,k\right]\Phi_{jo,k}\left[n\right] + \frac{1}{\sqrt{M}}\sum_{j=j_0}^{\infty}\sum_{k}W_{\psi}\left[j,k\right]\psi_{j,k}\left[n\right]\right] + \overline{P_{RX}}, \tag{6}$$

where $\overline{P_{RX}} = f(\overline{L})$. Equation (6) is represented in Figure 5.

3. Results and Discussion

In this section the results of the proposed model for the GSM channel are presented and discussed. The results were analyzed using Matlab® software in a dual core 2.4 GHz computer with a RAM of 4 GB.

Figure 6 presents the forecasted power values, with respect to those measured for one hour, for the wavelet neural model.

The availability time (it is the time interval that the channel is not used by the primary users and that could be used by CR users) and the occupancy time (it is the time interval that the channel is used by the primary users) of the measured and forecasted channel through the wavelet neural model are presented in Figures 7 and 8. The accuracy average obtained in the forecast of the availability time is 99.8%, and for the occupancy time it is equivalent to 99.9%.

In Table 3, the error criteria (symmetric mean absolute percentage error [SMAPE], mean absolute percentage error [MAPE], and mean absolute error [MAE]) are presented between real and forecasted data for the wavelet neural model. At the general level small errors are shown.

In Figure 9, the performance against the forecast is evaluated, from one to five days of wavelet neural model training. The error in the GSM channel forecast is reduced by a total of 1.75%, to the detriment of 31.24% in the observation time. Therefore, one training day for the wavelet neural model is sufficient to obtain an acceptable error.

Figure 10 shows the functioning of the proposed model. In this example the CR user perceives the power of a primary BS and may move over the cell coverage in the direction of the arrows. The CR user may forecast the power level that will be received from the primary BS at different distances, bearing in mind the environment propagation losses.

The evaluation of the proposed model covers the forecasting of up to one hour of received power, with a maximum distance of 328 m. The duty cycle over the analyzed environment is also presented.

By applying (6), the equation of the model in the proposed environment of Figure 2 is

$$P_{RX} = g\sum_{i=1}^{n}\left[\frac{1}{\sqrt{M}}\sum_{k}W_{\Phi}\left[j_0;k\right]\Phi_{jo;k}\left[n\right] + \frac{1}{\sqrt{M}}\sum_{j=j_0}^{\infty}\sum_{k}W_{\psi}\left[j;k\right]\psi_{j;k}\left[n\right]\right] + f\left[78.2616 + 26.16\log f_c - 13.82\log \text{hte} - a\left(h_{re}\right) + \left(19.5356 - 6.55\log \text{hte}\right)\log d\right]. \tag{7}$$

In Figure 11, (7) is graphed.

In Figure 11, the spectrum opportunities that would be perceived and profited by CR users are observable in orange color, although to be more precise they would depend on the selected threshold. These are obtained from the one-hour power forecast based on the historical information of one day. In Figure 11, the power level tends to decrease as the distance increases, according on the found losses.

In the example of Figure 10 the analysis of the proposed model is done by developing the power forecast from the CR user, using a similarity with the spectrum analyzer in which measurements were made. However, such similarity depends on the CR architecture deployed in the environment. Given that the processor and the power consumption are more limited in the device of the CR user, the use of an architecture with infrastructure is recommended, so that the forecast is developed from the CR BS. The CR BS is equipped with a better processor than the CR user and without limitations regarding power consumption.

Nevertheless, a period of time between the data collection in the environment and the processing adds a delay in the response that should not be ignored; but the forecast helps to reduce the negative impact of the delay in the response. In Figure 12 an architecture with infrastructure is shown [3].

For a CR system, the modeling developed in the channel of GSM band may contribute to improving the use of

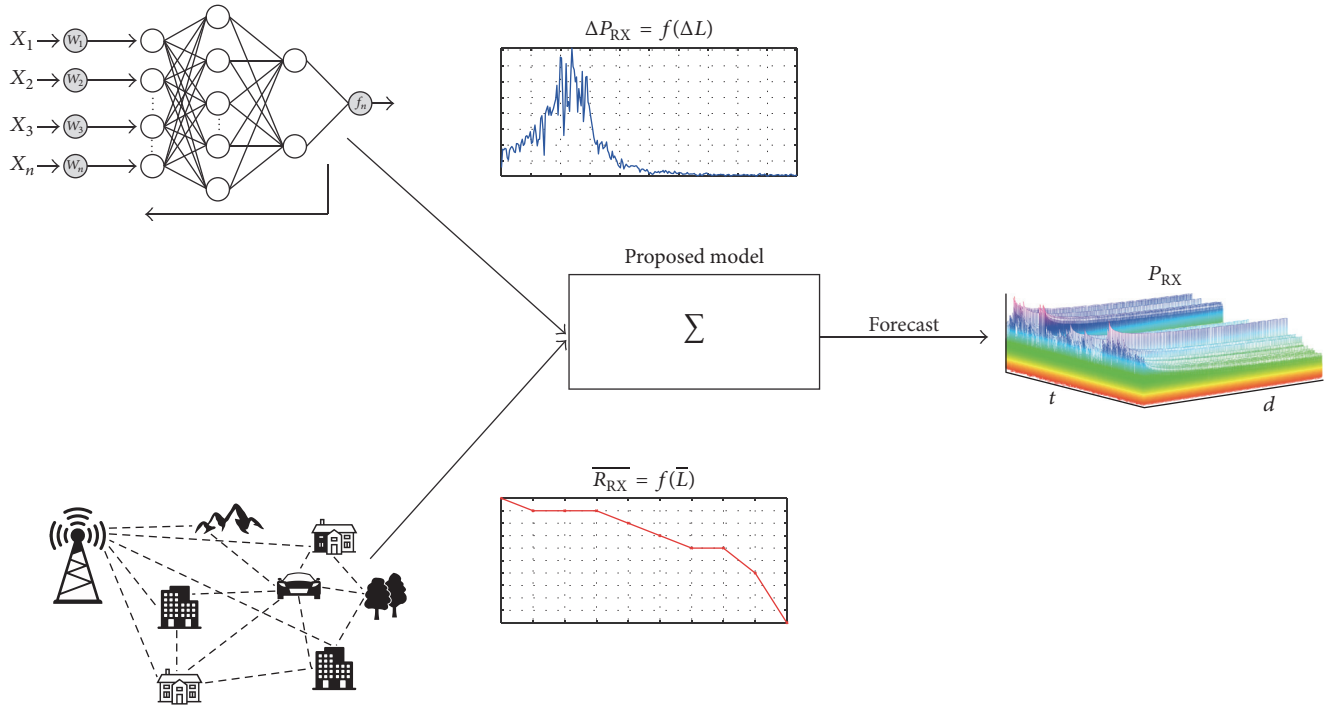

Figure 5: Scheme of the proposed model to forecast the spectrum opportunities.

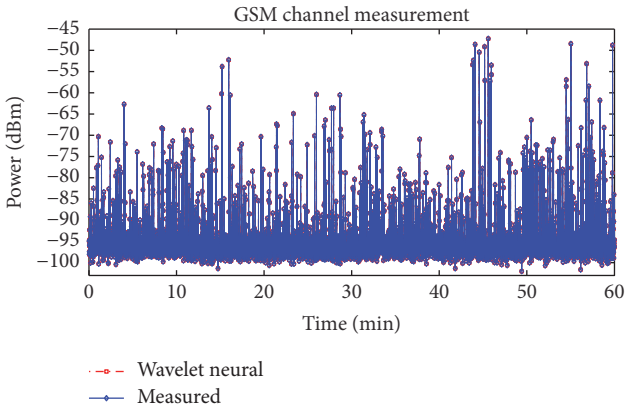

Figure 6: Measured and forecasted time series for GSM channels with the wavelet neural model.

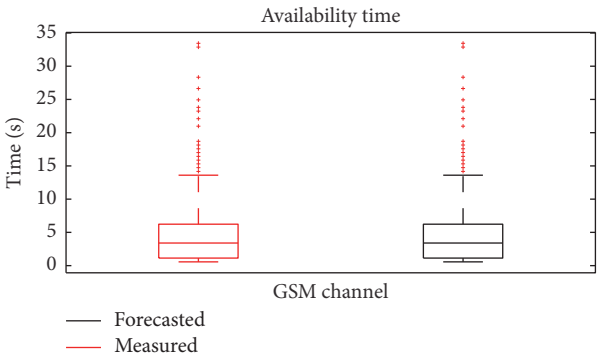

Figure 7: Availability time of forecasted GSM channel.

spectrum efficiency, as it allows CR users to share channels and to avoid collisions with primary users in the found spectrum opportunities.

3.1. Duty Cycle. The forecast of the duty cycle can be found using the following equation [15, 41]:

$$\psi = \left(1 - \sum_{k=1}^{K} \alpha_k\right) P_{\text{fa}} + \sum_{k=1}^{K} \alpha_k Q\left(\frac{Q^{-1}(P_{\text{fa}})\,\sigma_N - \gamma_k}{\sigma_{Sk}}\right), \quad (8)$$

where $K > 0$ represents the number of transmission power levels that can be present in the channel. In this case, in the measurements took on each spot of Figure 2 there is a single transmission power. $0 < \alpha_k \leq 1$ is the activity factor of the kth power level, which can be obtained from the average value of the use of the analyzed GSM channel. P_{fa} is the target probability of false alarm considered for the selection of the energy decision threshold, which in this case is of 1%. $\gamma_k = P_{\text{RX}k} - P_N$ is the signal to noise ratio resulting from the kth average transmission power level. σ_{Sk} and σ_N represent the standard deviation in decibels of the kth signal and noise power levels, respectively. These values were obtained experimentally using the spectrum analyzer and are presented in Table 4. $Q(\cdot)$ is the Gaussian Q-function and $Q^{-1}(\cdot)$ is the inverse of $Q(\cdot)$.

Table 4: Experimental values of σ_{Sk} and σ_N for GSM.

Band	B (kHz)	σ_{Sk} (dB)	σ_N (dB)
GSM	200	1.816	0.8785

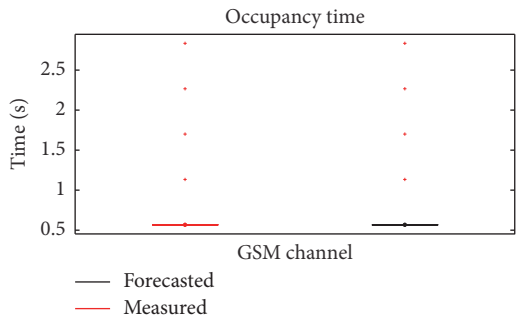

Figure 8: Occupancy time of forecasted GSM channel.

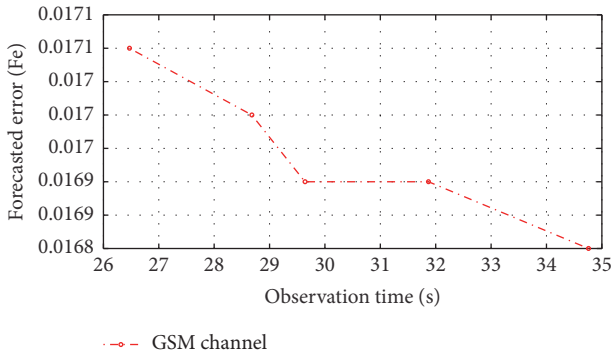

Figure 9: Forecast error versus observation time for the GSM channel.

P_{RXk} is the received power by the user, which has already been found for the proposed model, whereas P_N represents the CR terminal's noise floor created from the sum of all the noise sources in the receiver (including thermal noise) and can be expressed as follows:

$$P_N \text{ (dBm)} = -174 \text{ (dBm/Hz)} + 10 \log B \text{ (Hz)} + \text{NF (dB)}, \quad (9)$$

where −174 dBm/Hz is the thermal noise power spectral density at 290°K, B is the band width of the sensed channel, and NF is the total noise figure of the receiver. The noise figure of the low noise amplifier is 4 dB with a gain of 11 dB, and cable losses are of 0.72 dB. The noise figure of the analyzer is 16 dB for the implemented configuration. Thus, NF can be found by the total noise factor (F_T) [42]:

$$F_T = F_{ca} + \frac{F_{LNA} - 1}{G_{ca}} + \frac{F_{An} - 1}{G_{ca} G_{LNA}} = 3.266; \quad (10)$$

here, F_{ca} is the noise factor of the cable, F_{LNA} is the noise factor of the low noise amplifier, F_{An} is the noise factor of the spectrum analyzer, G_{ca} is the gain of the cable, and G_{LNA} is the gain of the low noise amplifier. Therefore, NF is 5.14 dB.

The duty cycle resulting from (8) for the proposed model in the sector of the BS cell of the exterior environment is shown in Figure 2.

Figure 13 shows that, as a result of the approach employed in (8), the scenario reveals different occupancy levels and not only busy or idle. For example, the probability of channel occupancy is low or high, but it is not equal to zero or one. In this way the performed modeling affords a realistic characterization of the spectrum occupancy forecast according to the considered propagation scenario, which constitutes a major aspect in the design and dimensioning of CR systems for real implementation.

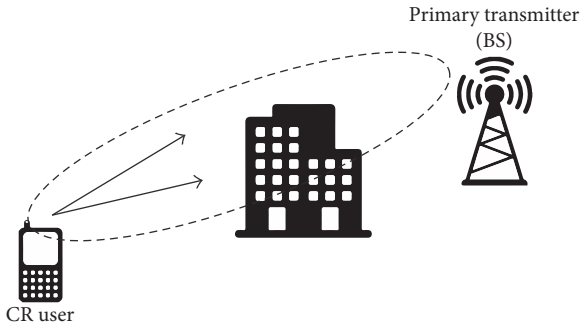

Figure 10: Application of the proposed model.

Figure 13 warns that the maximum occupancy levels fluctuate about 0.3. These values correspond to locations close to the BS and are graphed with the range of red colors. In general, occupancy values decrease and therefore the spectrum opportunities for CR users increase, as the signal moves away from the BS; such values are represented by the range of blue colors. This is consistent at a practical level and strengthens the proposed model.

4. Conclusions

In this study a model to forecast the spectrum opportunities was developed. The first step was the adjustment of the H-O propagation model with the measurements taken in an urban environment. Then, given the approximation of the adjustment and the average of the measured data, the integration with a wavelet neural model was performed.

The spectrum opportunities of the proposed model were set through the forecast of the received power in a determined time and the duty cycle within an urban environment. These results show the consistency with the practical behavior of the mobile communication systems.

The proposed methodology presents a novel and practical approach to forecasting the spectrum occupancy that would be perceived by CR users in real settings. The forecast of received power through propagation models is relevant as it allows CR users to access benefits such as saving energy in the spectrum sensing process, taking advantage of spectrum opportunities by increasing the successful transmission rate as well as the transmission opportunities, reducing the time to find available channels, and adjusting the transmission power levels to protect primary users from collisions and interferences.

Another advantage and difference is that whereas most of the forecast schemes are based on determining spectrum holes, the proposed methodology in this paper is based on an a priori knowledge of the received power by a channel

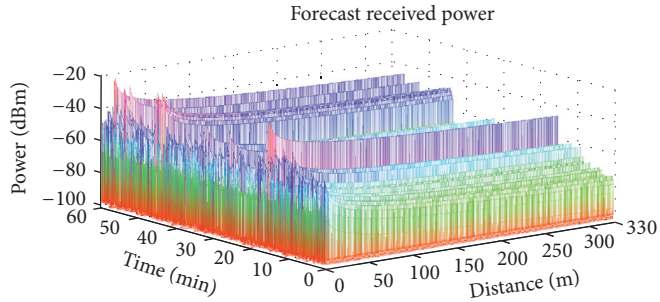

Figure 11: Forecast received power for the proposed model.

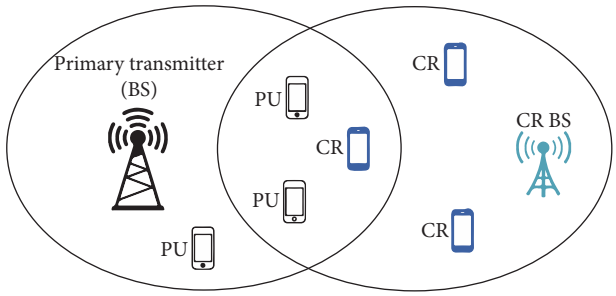

Figure 12: CR architecture with infrastructure.

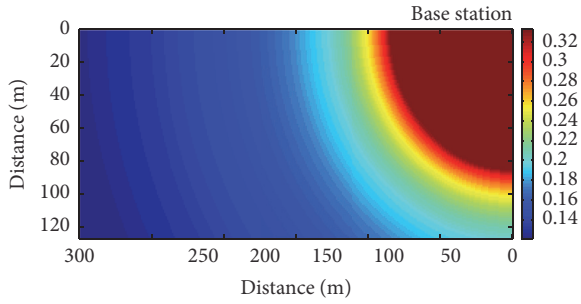

Figure 13: Duty cycle for the proposed model in the GSM channel.

of primary users, which facilitates the selection of nonnoisy channels and entails a better sharing of the spectrum among CR users. This leads to achieving superior quality of service parameters involving fewer radio resources.

Competing Interests

The authors declare that there is no conflict of interests regarding the publication of this paper.

References

[1] S. Haykin, "Cognitive radio: brain-empowered wireless communications," *IEEE Journal on Selected Areas in Communications*, vol. 23, no. 2, pp. 201–220, 2005.

[2] L. Pedraza, C. Hernandez, K. Galeano, and I. P. Páez, *Ocupación Espectral y Modelo de Radio Cognitiva para Bogotá*, Universidad Distrital Francisco José de Caldas, Bogotá, Colombia, 1st edition, 2016.

[3] I. F. Akyildiz, W.-Y. Lee, M. C. Vuran, and S. Mohanty, "NeXt generation/dynamic spectrum access/cognitive radio wireless networks: a survey," *Computer Networks*, vol. 50, no. 13, pp. 2127–2159, 2006.

[4] S. Rocke and A. M. Wyglinski, "Geo-statistical analysis of wireless spectrum occupancy using extreme value theory," in *Proceedings of the 13th IEEE Pacific Rim Conference on Communications, Computers and Signal Processing (PACRIM '11)*, August 2011.

[5] T. M. Taher, R. B. Bacchus, K. J. Zdunek, and D. A. Roberson, "Long-term spectral occupancy findings in Chicago," in *Proceedings of the IEEE International Symposium on Dynamic Spectrum Access Networks (DySPAN '11)*, pp. 100–107, Aachen, Germany, May 2011.

[6] F. H. Sanders, *Broadband Spectrum Survey at Los Angeles, California*, U.S. Department of Commerce National Telecommunications and Information Administration, Boulder, Colo, USA, 1997.

[7] M. Lõpez-Benítez and F. Casadevall, "Methodological aspects of spectrum occupancy evaluation in the context of cognitive radio," *European Transactions on Telecommunications*, vol. 21, no. 8, pp. 680–693, 2010.

[8] M. Wellens and P. Mähönen, "Lessons learned from an extensive spectrum occupancy measurement campaign and a stochastic duty cycle model," *Mobile Networks and Applications*, vol. 15, no. 3, pp. 461–474, 2010.

[9] K. Patil, K. Skouby, A. Chandra, and R. Prasad, "Spectrum occupancy statistics in the context of cognitive radio," in *Proceedings of the 14th International Symposium on Wireless Personal Multimedia Communications: Communications, Networking and Applications for the Internet of Things (WPMC '11)*, pp. 1–5, Brest, France, October 2011.

[10] D. Chen, S. Yin, Q. Zhang, M. Liu, and S. Li, "Mining spectrum usage data: a large-scale spectrum measurement study," in *Proceedings of the 15th Annual ACM International Conference on Mobile Computing and Networking (MobiCom '09)*, pp. 13–24, Beijing, China, September 2009.

[11] R. I. C. Chiang, G. B. Rowe, and K. W. Sowerby, "A quantitative analysis of spectral occupancy measurements for cognitive radio," in *Proceedings of the IEEE 65th Vehicular Technology Conference (VTC '07)*, pp. 3016–3020, Dublin, Ireland, April 2007.

[12] M. Mehdawi, N. G. Riley, M. Ammar, A. Fanan, and M. Zolfaghari, "Spectrum occupancy measurements and lessons learned in the context of cognitive radio," in *Proceedings of the 23rd Telecommunications Forum (TELFOR '15)*, pp. 196–199, Belgrade, Serbia, November 2015.

[13] A. Al-Hourani, V. Trajković, S. Chandrasekharan, and S. Kandeepan, "Spectrum occupancy measurements for different urban environments," in *Proceedings of the European Conference on Networks and Communications (EuCNC '15)*, pp. 97–102, Paris, France, July 2015.

[14] L. F. Pedraza, F. Forero, and I. Paez, "Metropolitan spectrum survey in bogota Colombia," in *Proceedings of the 27th International Conference on Advanced Information Networking and Applications Workshops (WAINA '13)*, pp. 548–553, Barcelona, Spain, March 2013.

[15] M. López-Benítez and F. Casadevall, "Statistical prediction of spectrum occupancy perception in dynamic spectrum access networks," in *Proceedings of the IEEE International Conference on Communications (ICC '11)*, pp. 1–6, Kyoto, Japan, June 2011.

[16] Y. Okumura, E. Ohmori, T. Kawano et al., "Field strength and its variability in UHF and VHF land-mobile radio service," *Review of the Electrical Communication Laboratory*, vol. 16, no. 9, pp. 825–873, 1968.

[17] G. L. Turin, F. D. Clapp, T. L. Johnston, S. B. Fine, and D. Lavry, "A statistical model of urban multipath propagation," *IEEE Transactions on Vehicular Technology*, vol. 21, no. 1, pp. 1–9, 1972.

[18] M. Hata, "Empirical formula for propagation loss in land mobile radio services," *IEEE Transactions on Vehicular Technology*, vol. 29, no. 3, pp. 317–325, 1980.

[19] J. Walfisch and H. L. Bertoni, "A theoretical model of UHF propagation in urban environments," *IEEE Transactions on Antennas and Propagation*, vol. 36, no. 12, pp. 1788–1796, 1988.

[20] D. Har, A. M. Watson, and A. G. Chadney, "Comment on diffraction loss of rooftop-to-street in COST 231-Walfisch-Ikegami model," *IEEE Transactions on Vehicular Technology*, vol. 48, no. 5, pp. 1451–1452, 1999.

[21] T. K. Sarkar, Z. Ji, K. Kim, A. Medouri, and M. Salazar-Palma, "A survey of various propagation models for mobile communication," *IEEE Antennas and Propagation Magazine*, vol. 45, no. 3, pp. 51–82, 2003.

[22] K. E. Stocker, B. E. Gschwendtner, and F. M. Landstorter, "Neural network approach to prediction of terrestrial wave propagation for mobile radio," *IEE Proceedings H: Microwaves, Antennas and Propagation*, vol. 140, no. 4, pp. 315–320, 1993.

[23] S. P. Sotiroudis, S. K. Goudos, K. A. Gotsis, K. Siakavara, and J. N. Sahalos, "Application of a composite differential evolution algorithm in optimal neural network design for propagation path-loss prediction in mobile communication systems," *IEEE Antennas and Wireless Propagation Letters*, vol. 12, pp. 364–367, 2013.

[24] E. Ostlin, H.-J. Zepernick, and H. Suzuki, "Macrocell path-loss prediction using artificial neural networks," *IEEE Transactions on Vehicular Technology*, vol. 59, no. 6, pp. 2735–2747, 2010.

[25] S. Phaiboon, P. Phokharatkul, and S. Somkuarnpanit, "2 to 16 GHz Microwave line-of-sight path loss prediction on Urban streets by fuzzy logic models," in *Proceedings of the IEEE Region 10 Conference (TENCON '05)*, pp. 1–4, Melbourne, Australia, November 2005.

[26] L. Pedraza, C. Hernandez, I. Paez, J. Ortiz, and E. Rodriguez-Colina, "Linear Algorithms for Radioelectric Spectrum Forecast," *Algorithms*, vol. 9, no. 4, article 82, 2016.

[27] S. Bai, X. Zhou, and F. Xu, ""Soft decision" spectrum prediction based on back-propagation neural networks," in *Proceedings of the IEEE International Conference on Computing, Management and Telecommunications (ComManTel '14)*, pp. 128–133, Da Nang, Vietnam, April 2014.

[28] S. Bai, X. Zhou, and F. Xu, "Spectrum prediction based on improved-back-propagation neural networks," in *Proceedings of the 11th International Conference on Natural Computation (ICNC '15)*, pp. 1006–1011, Zhangjiajie, China, August 2015.

[29] K. Lan, H. Zhao, J. Zhang, C. Long, and M. Luo, "A spectrum prediction approach based on neural networks optimized by genetic algorithm in cognitive radio networks," in *Proceedings of the 10th International Conference on Wireless Communications, Networking and Mobile Computing (WiCOM '14)*, pp. 131–136, Beijing, China, September 2014.

[30] S. Iliya, E. Goodyer, M. Gongora et al., "Optimized artificial neural network using differential evolution for prediction of RF power in VHF/UHF TV and GSM 900 bands for cognitive radio networks," in *Proceedings of the 14th UK Workshop on Computational Intelligence (UKCI '14)*, pp. 1–6, Bradford, UK, 2014.

[31] Y. Chen and H. S. Oh, "Spectrum measurement modelling and prediction based on wavelets," *IET Communications*, vol. 10, no. 16, pp. 2192–2198, 2016.

[32] L. Pedraza, C. Hernández, and I. Paez, "Evaluation of nonlinear forecasts for radioelectric spectrum," *International Journal of Engineering and Technology*, vol. 8, no. 3, pp. 1611–1626, 2016.

[33] L. F. Pedraza, C. A. Hernandez, and E. Rodriguez-Colina, "Study of models to forecast the radio-electric spectrum occupancy," *Indian Journal of Science and Technology*, vol. 9, no. 48, 2017.

[34] Q. Zhang and A. Benveniste, "Wavelet networks," *IEEE Transactions on Neural Networks*, vol. 3, no. 6, pp. 889–898, 1992.

[35] L. F. Pedraza, F. Forero, and I. P. Paez, "Evaluation Radioelectric Spectrum Occupancy in Bogota-Colombia," *Ingeniería y Ciencia*, vol. 10, no. 19, pp. 127–143, 2014.

[36] L. Debnath and F. Shah, *Wavelet Transforms and Their Applications*, Birkhäuser, New York, NY, USA, 2nd edition, 2014.

[37] A. F. Molisch, *Wireless Communications*, John Wiley & Sons, New York, NY, USA, 2nd edition, 2011.

[38] L. F. Pedraza, C. A. Hernandez, and E. Rodriguez-Colina, "A spectral opportunities forecasting method in a mobile network based on the integration of COST 231 Walfisch-Ikegami and wavelet neural models," *Contemporary Engineering Sciences*, vol. 10, pp. 113–128, 2017.

[39] T. S. Rappaport, *Wireless Communications: Principles and Practice*, Prentice-Hall, Upper Saddle River, NJ, USA, 2nd edition, 2002.

[40] K. Madsen, H. B. Nielsen, and O. Tingleff, *Methods for Non-Linear Least Squares Problems*, Informatics and Mathematical Modelling, Technical University of Denmark, Kongens Lyngby, Denmark, 2nd edition, 2004.

[41] M. Lopez and F. Casadevall, "Space-dimension models of spectrum usage for cognitive radio networks," *IEEE Transactions on Vehicular Technology*, vol. 66, no. 1, pp. 306–320, 2017.

[42] W. F. Egan, *Practical RF System Design*, John Wiley & Sons, Inc., Hoboken, NJ, USA, 1st edition, 2003.